

Carrier activation and mobility of boron-dopant atoms in ion-implanted diamond as a function of implantation conditions

J. R. Zeidler

*Naval Command, Control, and Ocean Surveillance Center, Research, Development, Test and Evaluation Division,
Code 804, 271 Catalina Boulevard, San Diego, California 92152-5000*

C. A. Hewett

*Naval Command, Control, and Ocean Surveillance Center, Research, Development, Test and Evaluation Division,
Code 555, 271 Catalina Boulevard, San Diego, California 92152-5000*

R. G. Wilson

Hughes Research Laboratories, 3011 Malibu Canyon Road, Malibu, California 90265

(Received 13 April 1992)

Natural type-IIa diamonds were implanted with either boron alone, carbon alone, or carbon plus boron at 77, 300, or 800 K. van der Pauw resistivity and Hall effect measurements of carrier concentration and mobility were made as a function of temperature to determine the most effective implantation conditions for semiconducting device applications. No measurable dopant incorporation occurs for the 800-K implant. The highest carrier concentration and mobility are observed when the implantation is carried out at 77 K. It is further shown that a significant increase in the hole concentration occurs when carbon is implanted prior to boron. These measurements provide direct confirmation of the theoretical predictions of Prins and co-workers. It is shown, however, that the carbon co-implant results in a decreased hole mobility. A multiple-step, low-temperature boron-ion implantation procedure that used three different implantation energies to produce an approximately uniformly doped *p*-type layer of about 200 nm thickness (as verified by secondary-ion-mass spectrometry on a separate sample) produced the best combination of carrier concentration and mobility. The resulting doped layer was used in the fabrication of an insulated-gate field-effect transistor that demonstrated current saturation and pinch-off at room temperature.

INTRODUCTION

Ion implantation is an important technology for semiconducting device applications because it provides an accurate method for controlling both the number and location of the dopant atoms. An extensive summary of the previous attempts to dope natural insulating diamond by using ion implantation has recently been provided by Prins and co-workers.¹⁻⁷ Prins and co-workers discuss the complexity of interpreting the implantation results due to the metastable nature of the diamond lattice. Much of the inconsistency in the reported results is attributed to the production of electrically active radiation damage due, in part, to the transformation of diamond bonds to graphitic bonds. It was shown that intrinsic radiation defects in diamond can act as donor, acceptor, or compensation centers which at high defect densities could produce impurity band electrical conduction via a hopping mechanism.⁸⁻¹⁰ Furthermore, implantation doses exceeding 5×10^{15} boron atoms per cm^2 result in the irreversible transformation of diamond bonds to graphitic bonds during annealing.^{10,11}

Prins⁴ proposed that the percentage of implanted boron atoms that are incorporated into the diamond lattice on substitutional sites can be increased by performing the implantation at low temperature (77 K in Refs. 1-4) to inhibit the migration of the interstitials out of the im-

planted region. Prins further proposed⁴ that a low-temperature implantation of carbon ions in a prescribed ratio relative to the boron ion dose would create a vacancy-rich region for the subsequent boron implantation and annealing procedures. During a rapid post implant anneal, the recombination of the self-interstitials and vacancies reduces radiation damage while boron combining with vacancies produces electrically active dopant incorporation. This was indicated in Ref. 4 by optical transmission and electrical resistance measurements of diamonds implanted with various ratios of carbon and boron ions. Further confirmation was obtained by Sandhu, Swanson, and Chu¹² by using additional optical absorption and electrical resistance measurements of natural insulating (type IIa) diamonds that were co-implanted with boron and carbon ions.

Liu *et al.*¹³ refined the critical carbon ion implantation dose for irreversible lattice damage in diamond by using Rutherford backscattering spectrometry (RBS) and ion channeling measurements. It was shown that for 200 keV carbon atoms implanted at 77 K, diamond is amorphized at a critical dose between 1.65×10^{15} and 3×10^{15} cm^{-2} . It was further shown¹³ that below this critical dose, epitaxial regrowth of the radiation damage could be accomplished by either rapid thermal annealing (RTA) or furnace annealing; above this dose, furnace annealing up to 1173 K produced a nearly perfect crystal in the epitax-

ially regrown region, whereas RTA resulted in poor crystallinity. An analysis of the depth distributions of ^{13}C , ^{11}B , and ^7Li atoms implanted into natural type-Ia and type-IIa diamonds at temperatures ranging between 90 and 670 K was provided by Spits *et al.*¹⁴ Nuclear reaction profiling in conjunction with RBS and ion channeling measurements was used to study the interaction and redistribution of dopant atoms and displaced carbon atoms during the implantation and annealing processes. Nuclear reaction analysis clearly showed that the amount of boron trapped in the damaged region decreased as the implantation temperature was increased.¹⁴

More recently, Prins^{1,2} has shown that the carbon self-interstitial-vacancy recombination rate and the boron interstitial-vacancy combination rate exhibit different dependencies on the annealing temperature, rather than the simple equireate models assumed in Refs. 3 and 4. The sheet resistance for diamond implanted with a fixed carbon dose was demonstrated to increase by over seven orders of magnitude as the annealing temperature was increased from 1123 to 1348 K. The self-interstitial-vacancy recombination rates increased continuously with increasing annealing temperature throughout this temperature interval. For boron-implanted diamond, however, the sheet resistance is at a minimum for an annealing temperature of approximately 1273 K, and increases by over five orders of magnitude as the annealing temperature is increased from 1273 to 1373 K. This indicates that the boron acceptor activation efficiency is maximized by annealing the implanted samples at approximately 1273 K. Subsequent annealing at higher temperatures can then provide for further reductions in the radiation damage.

In this paper we investigate the implantation conditions that provide the best characteristics for diamond electronic device applications. Device applications require not only the low sheet resistance produced by electrically active substitutional boron atoms in the diamond lattice, but also a high hole mobility. Direct measurements of both the carrier concentration and the hole mobility are made as a function of temperature for natural type-IIa diamond implanted with either boron or carbon, or co-implanted with boron and carbon, at substrate temperatures of 77, 300, or 800 K. The sample demonstrating the best combination of carrier concentration and mobility was then used to provide the conducting layer for an insulated-gate field-effect transistor.

EXPERIMENTAL PROCEDURE

Natural type-IIa diamonds, $5 \times 5 \times 0.25 \text{ mm}^3$ or $4 \times 4 \times 0.25 \text{ mm}^3$ in size, with a (100) orientation, were used throughout this study. The implantation conditions were selected to allow verification of the approach suggested by Prins.⁴ In both cases trilevel implant procedure was used to provide an approximately uniformly doped *p*-type layer of about 200 nm in thickness, as predicted by transport of ions in materials (TRIM) (6.04) calculations and as subsequently confirmed by secondary-ion-mass spectrometry (SIMS) measurements performed at Charles Evans & Associates on a separately implanted test sam-

ple. Depth distributions and range parameters for boron and other elements in diamond are provided in Ref. 15. Implantation of ^{11}B and ^{12}C was performed in a 400 kV custom ion implanter at Hughes Research Laboratories. ^{11}B ions were produced from BF_3 gas in an electron-bombardment ion source; ^{12}C ions were produced from a CO gas source. The ion beam was mass separated at full energy by using a double focusing magnet. Neutral particles were removed and the beam electrostatically scanned to provide a uniform implant at 7° from the (100) axis. The fluence was determined by integrating the net positive charge striking the target, which is biased and isolated from ground potential through a current integrator. SIMS was used to verify the measured fluences in separate calibration runs. The target chamber was evacuated to about 10^{-6} Torr using a cryopump. The diamonds were mounted on a temperature-controlled sample holder for the specified implantation conditions. Six diamonds were implanted at the temperatures, doses, and conditions indicated in Table I. Ion current densities were controlled to complete the desired implantation dose in time intervals between 60 and 600 s.

After implantation, the samples were immediately removed from the implantation stage, placed in a quartz furnace preheated to 1263 K, and annealed under flowing dry nitrogen to remove implantation damage and activate the implanted boron. In all but one case the annealing time was 10 min. For the low dose, low-temperature boron-only implantation, a 60 min anneal was used to determine whether additional annealing time would improve the activation efficiency and mobility. For the 10 min anneals, a visual change in the color of the implanted samples was evident after annealing. Prior to the anneal, the surface exhibited a light bronze coloration and a shadow was apparent in the region that had been masked by the sample holder clip during implantation. After annealing, the surface was clear and the region masked by the clip was no longer evident. After the 60 min anneal, however, the surface was blackened. The diamonds were then transported to Naval Command, Control, and Ocean Surveillance Center, Research, Development, Test and Evaluation Division where all subsequent processing was done. The samples were first cleaned by etching in a boiling saturated solution of CrO_3 in sulfuric acid to remove any potential graphitized layers resulting from the implantation process. The diamonds were then rinsed in deionized water, boiled in acetone, rinsed with methanol, then blown dry by using dry nitrogen. After this procedure, all of the diamonds, including the sample that had been blackened during the 60 min anneal, appeared clear and free of visible radiation damage. The samples were then loaded into an ultrahigh vacuum chamber for Ohmic contact metallization. The base pressure of the chamber was approximately 1×10^{-8} Torr.

Contacts were evaporated onto the sample corners by using a stainless-steel shadow mask. The contact metallization consisted of 10 nm of Mo deposited by electron-beam evaporation, followed by 150 nm of Au deposited from a resistively heated boat. After removal from the vacuum chamber, the samples were baked at 393 K for 20 min, then annealed for 6 min at 1233 K in a dry hy-

drogen ambient (dew point less than 210 K). The effect of this additional annealing on the activation of the boron, or on the annealing of implantation-induced defects, should be minimal as the contact annealing temperature is 30° lower and the contact anneal time is 6 vs 10 min for the activation anneal. The electrical contacts produced by this process have been extensively characterized in previous studies.¹⁶⁻²⁰ The formation of carbide precipitates at the diamond-metal interface during the anneal leads to Ohmic contacts with low specific contact resistance and high mechanical integrity.^{17,18} The long-term reliability of these contacts has been demonstrated at temperatures between 723 and 898 K for time intervals in excess of 130 h.¹⁹ Gold wires were then wire bonded between the Mo/Au evaporated contacts and the gold contact pads of a chip carrier and mounted in the high-temperature van der Pauw resistivity and Hall-effect measurement apparatus shown in Fig. 1.

Initial measurements^{19,21} revealed that it was necessary to control the ambient atmosphere in which the transport measurements were made in order to inhibit high-temperature surface interactions between diamond and gas species such as oxygen and hydrogen.^{22,23} High-purity argon was generated by using a purifier system that employs hot Ti chips and fed into the system that was maintained at a dew point of less than 158 K (as monitored by a hygrometer in the gas exhaust line). The sample was radiatively heated by furnace coils surrounding the quartz chamber. The temperature was controlled by a Variac attached to the furnace coils and was monitored by a thermocouple inserted in a socket below the

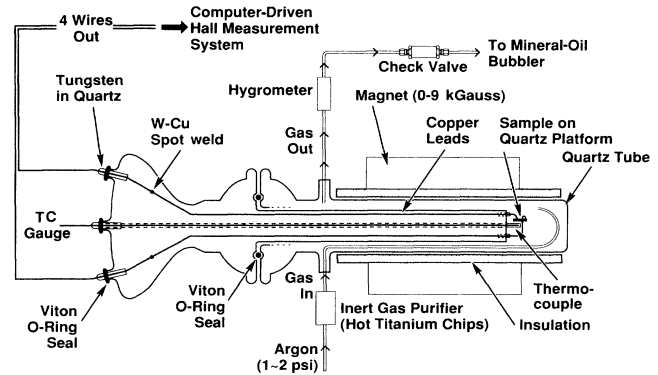


FIG. 1. Apparatus for high-temperature van der Pauw resistivity and Hall-effect measurements in a controlled ambient. (The TC gauge is a thermocouple for temperature control.)

sample platform. The samples were heated to a maximum temperature of 1058 K and resistivity and Hall effect measurements were then made as a function of temperature.

The van der Pauw resistivity measurements evaluate the voltage induced across two adjacent corner contacts for a measured current between the remaining two contacts. The I - V measurements are then repeated for all pairs of contacts to increase accuracy and evaluate the sample homogeneity. Similarly, the Hall data consist of measurements of the voltage across two diagonally opposing corner contacts for a defined current between the other pair of corner contacts with a magnetic field per-

TABLE I. Ion-implantation conditions.

Implant species	Ion energy (kev)	Implant dose (cm ⁻²)	Implant temperature (K)	Anneal time (min)
¹² C ⁺	120	3.0 × 10 ¹⁴	77	10
	60	2.1 × 10 ¹⁴		
	30	1.5 × 10 ¹⁴		
¹² C ⁺ + ¹¹ B ⁺	120	3.0 × 10 ¹⁴	77	10
	60	2.1 × 10 ¹⁴		
	30	1.5 × 10 ¹⁴		
	100	3.0 × 10 ¹⁴		
	50	2.1 × 10 ¹⁴		
	25	1.5 × 10 ¹⁴		
¹¹ B ⁺	100	3.0 × 10 ¹⁴	77	10
	50	2.1 × 10 ¹⁴		
	25	1.5 × 10 ¹⁴		
¹¹ B ⁺	100	3.0 × 10 ¹³	77	60
	50	2.1 × 10 ¹³		
	25	1.5 × 10 ¹³		
¹¹ B ⁺	100	3.0 × 10 ¹⁴	300	10
	50	2.1 × 10 ¹⁴		
	25	1.5 × 10 ¹⁴		
¹¹ B ⁺	100	3.0 × 10 ¹⁴	800	10
	50	2.1 × 10 ¹⁴		
	25	1.5 × 10 ¹⁴		

pendicular to the plane of the sample. Initial room-temperature calibration measurements were made with probe wires attached to the evaporated contact pads with In solder. Significant improvements in both the van der Pauw function and the magnitudes of the induced van der Pauw voltages were obtained for the wire bonded contact procedure described above. Measurements were carried out in a magnetic field of 0.95 T with injected currents varied between 1 nA and 10 μ A.

RESULTS AND DISCUSSION

The sheet resistance data shown in Fig. 2 indicate that the lowest resistance is achieved by co-implanting with carbon and boron at low temperature. The resistance for this sample is more than an order of magnitude lower than that of the sample implanted with boron alone at low temperature. The sample implanted with an order-of-magnitude lower boron dose, but annealed for 60 min, exhibited a significantly increased resistance but was still superior to that obtained for the sample implanted with a full boron dose at 300 K. The room-temperature boron implant produced a lower sheet resistance than the low-temperature carbon-only implant, while the 800 K boron-only implant exhibited the highest sheet resistance among all the implanted samples. The fact that the high-temperature boron-only implant produces the highest resistance corroborates the nuclear reaction analysis results in Ref. 14 which showed, by direct boron depth profiling, that most of the boron implanted at 670 K migrated out of the implant region. In addition, Ref. 14 shows that while boron implantation at 370 K results in a somewhat greater concentration of boron in the implant region than does implantation at 670 K, implantation of boron at 90 K results in significantly greater boron concentrations than either the 370 or 670 K implantations. The increased sheet resistance of the 800 K boron-only implantation over the low-temperature carbon-only implantation observed in this work is presumably caused by a reduction in electrically active

lattice defects produced in the course of the high-temperature implant, thus indicating that the 10 min activation anneals do not remove all the residual lattice damage. Prins¹⁻⁴ showed that after a 60 min anneal at 1271 K to activate the boron, a higher-temperature anneal over a longer time period will further reduce the number of residual defects.

The carrier concentration data, summarized in Fig. 3, indicates that the low-temperature carbon plus boron co-implantation procedure produces an increase in the total number of holes of almost two orders of magnitude over that obtained with boron alone. The reduced dose boron implant does provide fewer carriers, but due to the increased annealing time, the amount of reduction is less than the order-of-magnitude decrease expected from the decrease in the dose. The 300-K boron-only implant produced a measurable hole concentration, but the density was approximately an order of magnitude lower than that of the sample implanted with an equal boron dose at 77 K. Neither the sample that was implanted with carbon only at 77 K nor the sample implanted with B only at 800 K produced a measurable carrier concentration.

Collins, and co-workers²⁴⁻²⁶ discuss the use of the carrier-concentration curves to compute the free hole, donor, and acceptor concentrations and the hole activation energy in both natural and in synthetic diamonds (the synthetic diamonds analyzed were grown by a high-temperature, high-pressure technique). It was shown that for natural diamond with hole concentrations on the order of 3×10^{16} cm⁻³, a single-hole activation energy can be readily extracted from the temperature dependence of the variation of $N_A - N_D$. For synthetic type-IIb diamond with acceptor concentrations between 10^{17} and 10^{19} cm⁻³, however, the carrier concentration depended on three independent conductivity mechanisms, all with different activation energies that produced different temperature dependences for different samples.^{24,26} For ion-implanted samples other defect-induced conductivity mechanisms are also possible, making the interpretation of the carrier-concentration curves even more difficult.

The concentration of boron atoms in the active layer

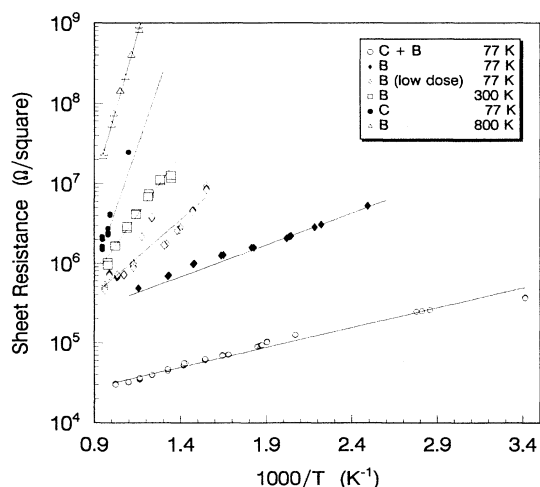


FIG. 2. Sheet resistance as a function of inverse temperature for the implantation conditions specified in Table I.

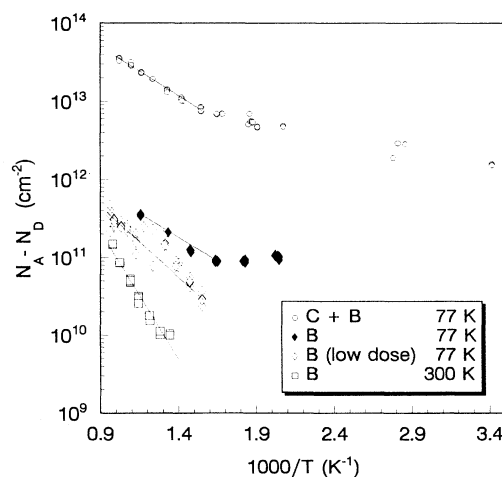


FIG. 3. Net carrier concentration as a function of inverse temperature for the implantation conditions of Table I.

TABLE II. TRIM simulation results.

Ion	Energy (keV)	R_p (nm)	ΔR_p (nm)	R_D (nm)	Vacancies per ion
^{12}C	120	162.5	25.7	151.6	114.9
^{12}C	60	87.9	18.2	75.0	87.9
^{12}C	30	46.1	12.1	35.9	63.3
^{11}B	100	173.7	28.0	159.4	100.5
^{11}B	50	93.2	19.7	81.3	77.2
^{11}B	25	48.5	13.0	37.5	55.7

for these measurements is on the order of $3 \times 10^{19} \text{ cm}^{-3}$, and within the general range of the synthetic diamonds analyzed in Ref. 26. An analysis of the low-temperature, full-dose, boron-only implantation was provided in Ref. 21. It is shown that the slope of $\ln(p)$ vs $(1/kT)$ between 600 and 850 K corresponds to an energy of 0.29 eV. Depending on the assumptions made about the degree of compensation in the active region, these data imply an acceptor binding energy of between 0.18 and 0.49 eV Ref. 21. This binding energy is in agreement with the results of Vavilov *et al.*²⁷ who reported a boron-ionization energy of 0.19 eV under the assumption that $p \ll N_D$.

The carrier mobility results in Fig. 4 show that the carbon plus boron co-implanted sample exhibits a significant decrease in the hole mobility relative to samples implanted with boron alone. In all cases the measurements showed considerable variation, but repeated trials and repeated measurements at each temperature were used to obtain reliable data. The noticeably greater scatter in the mobility data is attributed to the fact that mobility is derived from the measured sheet resistance and the measured carrier concentration, and therefore contains the errors of both measurements. Again, neither the carbon-only implant nor the 800 K boron implant produced a measurable hole mobility.

In initial calibration runs of the system, van der Pauw resistivity and Hall effect measurements were made on a natural type-IIb semiconducting diamond. The tempera-

ture dependence of the free hole concentration vs temperature was equivalent to that obtained by Collins and co-workers^{24,25} and indicated a hole activation energy of 0.33 eV. The measured mobility of this sample was $400 \text{ cm}^2 \text{ V}^{-1} \text{ s}^{-1}$ at 300 K. This is lower than the values reported in Refs. 24 and 25 but within the range reported by others^{28,29} for synthetic diamond. The lower mobility values may be indicative of a higher defect density in our sample relative to that measured in Ref. 25. Vavilov *et al.*²⁷ reported room-temperature mobilities of between 200 and $700 \text{ cm}^2 \text{ V}^{-1} \text{ s}^{-1}$ for natural diamond implanted with 40-keV boron ions at room temperature and vacuum annealed at 1673 K for 2 h. Consequently, it is reasonable to expect that a better optimized set of implantation and annealing conditions would improve the hole mobility.

Since the sample implanted with carbon plus boron received a total implant dose twice that of the sample implanted with boron alone this reduction in mobility is not surprising. With the increase in activation associated with the carbon preimplant, however, this might be controlled by reducing both the carbon and boron implant doses. Alternatively, as discussed below, it might be possible to design an equally effective implantation scheme using suitably tailored multienergy boron-only implants.

Shown in Table II are the summarized results of the TRIM simulations for carbon or boron implanted into diamond. It is clear that boron and carbon are approximately equal in vacancy creation efficiency; even with the 20% difference in energy (120 keV vs 100 keV, etc.) the vacancies per ion differ by only 10–15%. This suggests that the use of carbon for the co-implantation might be unnecessary for a multienergy implant. If the implants are carried out in order of descending energies, each implant leaves a defect profile for subsequent implants similar to that of a carbon preimplant. In addition to reducing the number of implantations required, this procedure also eliminates the additional interstitial carbon atoms that make no useful contribution to the desired boron-vacancy combination process.

The simulation results also show that the energies selected were not the optimal choices to enhance boron-vacancy interactions. In each case the boron projected range (R_p) is approximately 15–35% greater than the maximum in the damage profile (R_D). For the maximum number of boron-vacancy combinations R_p should coincide with R_D . In the case of a multienergy boron-only implant, R_p for each energy should coincide with R_D from the previous energy implant.

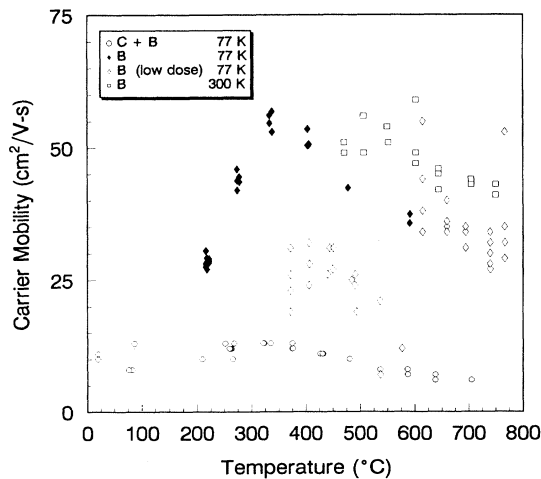


FIG. 4. Hole mobility as a function of temperature for the implantation conditions of Table I.

DEVICE FABRICATION USING ION IMPLANTATION

To investigate the effectiveness of ion implantation for electronic device applications, the sample implanted with the full boron dose at low temperature (without a carbon preimplant) was used to fabricate an insulated gate field-effect transistor. (Due to its higher carrier concentration the carbon preimplanted sample had promising device potential. Unfortunately, the layer was destroyed in processing and a direct comparison is not possible.) This structure was selected to eliminate the gate leakage problem observed in diamond metal-semiconductor field-effect transistor fabrication.³⁰ A circular geometry that consisted of a central drain contact 400 μm in diameter, with concentric 200- μm -wide gate and source contacts 1000 and 1600 μm in diameter, was chosen to eliminate the need for a mesa etch. Removal of the Mo/Au contacts used for the van der Pauw resistivity and Hall effect measurements, and of any residual damaged layers on the diamond surface, was accomplished by again immersing the sample in a boiling saturated solution of CrO_3 in sulfuric acid. The Ohmic source and drain contacts, consisting of a bilayer structure of 10 nm of Mo deposited on the diamond and capped with 160 nm of Au, were defined by a lift-off process^{17,31} and annealed at 1223 K in a dry hydrogen environment. The gate insulator, consisting of an SiO_2 film approximately 100 nm thick, was deposited by indirect plasma-enhanced chemical vapor deposition at a temperature of 573 K. The gate metal, also defined by a lift-off process, was a 10-nm Ti/160-nm Au bilayer structure.³¹ Ti was selected as the gate metal to provide good adhesion to the gate insulator, with the Au cap to prevent oxidation of the Ti and to lower the gate resis-

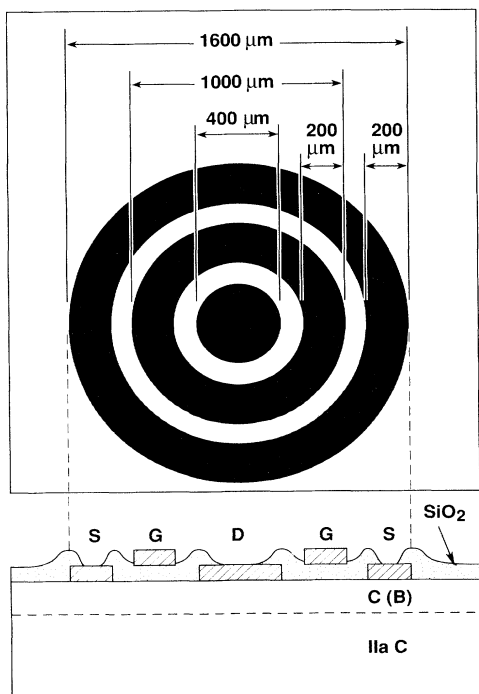


FIG. 5. Schematic outline of the transistor structure.

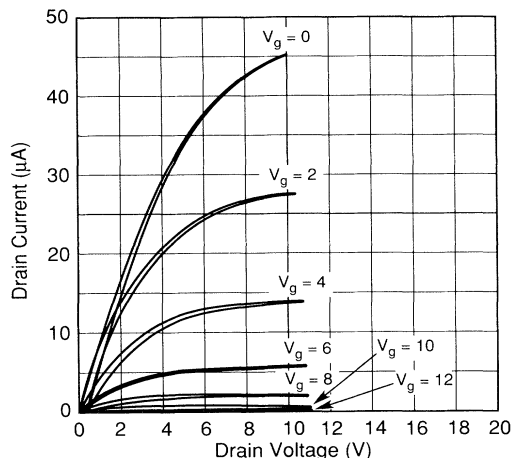


FIG. 6. Room-temperature transistor characteristics of the device shown schematically in Fig. 5.

tance. All metallizations were deposited in an ultrahigh vacuum system with a pressure during deposition of less than 7×10^{-8} Torr.

A cross-sectional view of the resulting device structure is shown in Fig. 5. The room-temperature transistor characteristics were then obtained for fixed gate voltages V_G between 0 and 12 V. As shown in Fig. 6, drain current saturation is observed over the entire range of V_G and current pinch-off is achieved between gate voltages of 10 and 12 V. Additional details on the device fabrication and performance are provided in Ref. 31.

CONCLUSIONS

It was shown that the sheet resistance of the implanted samples agrees with the previous results,^{1-4,12} and that the use of a carbon implant prior to boron implantation produces an increase in the number of activated boron atoms of almost two orders of magnitude over that obtained with boron implantation alone. This is a direct confirmation of the methodology developed in Refs. 1-4. It is shown, however, that the hole mobility in the carbon plus boron co-implanted sample was significantly reduced relative to the sample implanted with boron alone. The sample implanted at 800 K had the highest sheet resistance of all implanted samples (even higher than the low-temperature carbon implant) and produced no measurable carriers. This result is in agreement with the nuclear reaction profiling results in Ref. 14 that show that the implanted boron quickly migrates from the implanted region for a high-temperature implant. It is of interest to investigate alternate procedures where multienergy boron implants are used instead of carbon implants to produce the vacancy-rich region for subsequent boron implantations, thereby replacing excess interstitial carbon atoms, which can make no useful contribution to the desired boron-vacancy combination, with additional boron interstitials. It is clear that an extended annealing time at a higher temperature would reduce the concentration of defects in the active layer and improve both carrier mobility and device performance. Nonetheless, it was shown that effective transistor action can be obtained

from a device based on the ion implantation procedures utilized.

ACKNOWLEDGMENTS

The authors gratefully acknowledge the contributions of Dr. Paul de la Houssaye, Dr. Mark Roser, and Professor Claude Penchina in constructing the high-temperature electrical transport measurement system and in performing some of the initial measurements. The authors further acknowledge the assistance of Dr. Carl

Zeisse and Richard Nguyen in fabricating the device structure and for other contributions. The assistance of Marylin Taylor, Dr. Donald Mullin, Professor Khos Moazed, and Dr. Howard Rast is also acknowledged. This research was supported by the Naval Ocean Systems Center (now NCCOSC, RDT&E Div.). The electrical contact procedures used here were developed under funding from the Office of Naval Research. The authors would also like to acknowledge Dr. Michael Seal of Sigillum, B.V., and Drukker International, B.V., for the loan of samples used in this work.

-
- ¹J. F. Prins, Phys. Rev. B **44**, 2470 (1991).
²J. F. Prins, Nucl. Instrum. Methods B **59**, 1387 (1991).
³J. F. Prins, Phys. Rev. B **39**, 3764 (1989).
⁴J. F. Prins, Phys. Rev. B **38**, 5576 (1988).
⁵J. F. Prins, Nucl. Instrum. Methods B **35**, 484 (1988).
⁶J. F. Prins, T. E. Derry, and J. P. F. Sellschop, Phys. Rev. B **34**, 8870 (1986).
⁷J. F. Prins, Phys. Rev. B **31**, 2742 (1985).
⁸J. J. Hauser and J. R. Patel, Solid State Commun. **18**, 789 (1967).
⁹J. J. Hauser, J. R. Patel, and J. W. Rodgers, Appl. Phys. Lett. **30**, 129 (1977).
¹⁰R. Kalish, T. Bernstein, B. Shapiro, and A. Talmi, Radiat. Eff. **52**, 153 (1980).
¹¹V. S. Vavilov, V. V. Krasnopevtsev, and Yu. V. Milyutin, Radiat. Eff. **22**, 141 (1974).
¹²G. S. Sandhu, M. L. Swanson, and W. K. Chu, Appl. Phys. Lett. **55**, 1397 (1989).
¹³B. Liu, G. S. Sandhu, N. R. Parikh, and M. L. Swanson, Nucl. Instrum. Methods B **45**, 420 (1990).
¹⁴R. A. Spits, T. E. Derry, J. F. Prins, and J. P. F. Sellschop, Nucl. Instrum Methods B **59/60**, 1366 (1991).
¹⁵R. G. Wilson, Surf. Coat. Tech. **47**, 559 (1991).
¹⁶K. L. Moazed, R. V. Nguyen, and J. R. Zeidler, IEEE Electron Device Lett. **9**, 350, (1988).
¹⁷K. L. Moazed, J. R. Zeidler, and M. J. Taylor, J. Appl. Phys. **68**, 2246 (1990).
¹⁸C. A. Hewett and J. R. Zeidler, Diamond and Related Mater. **1**, 688 (1992).
¹⁹M. Roser, C. A. Hewett, K. L. Moazed, and J. R. Zeidler, J. Electrochem. Soc. **139**, 2001 (1992).
²⁰J. R. Zeidler and K. L. Moazed, U.S. Patent No. 5,055,424 (8 October 1991).
²¹P. R. de la Houssaye, C. Penchina, C. A. Hewett, J. R. Zeidler, and R. G. Wilson, J. Appl. Phys. **71**, 3220 (1992).
²²M. I. Landstrass and K. V. Ravi, Appl. Phys. Lett. **55**, 975 (1990).
²³S. Albin and L. Watkins, IEEE Electron Device Lett. **11**, 159 (1990).
²⁴A. T. Collins and E. C. Lightowers, in *The Properties of Diamond*, edited by J. E. Field (Academic, New York, 1979), pp. 79–109.
²⁵A. T. Collins and A. W. S. Williams, J. Phys. C. **4**, 1789 (1971).
²⁶A. W. S. Williams, E. C. Lightowers, and A. T. Collins, J. Phys. C. **3**, 1727 (1970).
²⁷V. S. Vavilov, M. A. Gusasyan, M. I. Guseva, T. A. Karatygina, and E. A. Konorova, Sov. Phys. Semicond. **8** (4), 471 (1974).
²⁸N. Fujimori, H. Nakahata, and T. Imai, Jpn. J. Appl. Phys. **29** (5), 824 (1990).
²⁹P. I. Baranskii, V. G. Malogolvets, V. I. Torishnii, and G. V. Chipenko, Sov. Phys. Semicond. **21** (1), 45 (1987).
³⁰G. Sh. Gildenblat, S. A. Grot, C. W. Hatfield, and A. R. Badzian, IEEE Electron Device Lett. **12**, 37 (1991).
³¹C. R. Zeisse, C. A. Hewett, R. Nguyen, J. R. Zeidler, and R. G. Wilson, IEEE Electron Device Lett. **12**, 602 (1991).